

MATHEMATICAL ENGINEERING TECHNICAL REPORTS

Formation Control of Multi-Agent Systems with Sampled Information

— Relationship Between Information Exchange
Structure and Control Performance —

Tomohisa Hayakawa, Takuji Matsuzawa,
and Shinji Hara

(Communicated by Kazuo MUROTA)

METR 2006-55

November 2006

DEPARTMENT OF MATHEMATICAL INFORMATICS
GRADUATE SCHOOL OF INFORMATION SCIENCE AND TECHNOLOGY
THE UNIVERSITY OF TOKYO
BUNKYO-KU, TOKYO 113-8656, JAPAN

WWW page: <http://www.i.u-tokyo.ac.jp/mi/mi-e.htm>

The METR technical reports are published as a means to ensure timely dissemination of scholarly and technical work on a non-commercial basis. Copyright and all rights therein are maintained by the authors or by other copyright holders, notwithstanding that they have offered their works here electronically. It is understood that all persons copying this information will adhere to the terms and constraints invoked by each author's copyright. These works may not be reposted without the explicit permission of the copyright holder.

Formation Control of Multi-Agent Systems with Sampled Information

— Relationship Between Information Exchange
Structure and Control Performance —

Tomohisa Hayakawa[†], Takuji Matsuzawa[‡], and Shinji Hara[‡]

[†]Department of Mechanical and Environmental Informatics
Graduate School of Information Science and Engineering
Tokyo Institute of Technology
`tomohisa_hayakawa@ipc.i.u-tokyo.ac.jp`

[‡]Department of Information Physics and Computing
Graduate School of Information Science and Technology
The University of Tokyo
`{takuji_matsuzawa, shinji_hara}@ipc.i.u-tokyo.ac.jp`

November 15, 2006

Abstract

A problem of controlling multi-agent systems with intermittent information exchange between the agents is considered. Through energy-based analysis, we first derive stability conditions given a communication network structure and a sampling period. Furthermore, we relate the network topology and control performance in terms of the system's aggregate energy dissipation rate.

1 Introduction

There has been a great deal of interest in controlling large-scale dynamical systems composed of multiple mobile agents. The framework of multi-agent systems has variety of applications such as air traffic control [1], intelligent highways [2], multiple robots carrying out cooperative tasks [3], coordinated control of satellites for Earth observation [4], RoboCup Soccer [5], to cite but a few examples and references. One of the key issues in those systems is the requirement of decentralized control architecture [6] so that each agent can determine its own control signals without necessarily monitoring the states of the overall agents. In this sense it is important to construct a proper

communication network of information exchange between the agents such that the aggregate system fulfills prescribed tasks with good performance.

In 1987, Reynolds published a remarkable paper that deals with the collective movement of objects mimicking a flock of birds in the area of computer animation [7]. His algorithm was predicated on the three rudimentary principles, that is, separation, alignment, and cohesion of the agents, for expressing the emergent behavior without any leader-follower distinctions. In [8], Vicsek *et al.* considered biologically inspired cooperative formation of self-driven particles in the discrete-time setting and their simulation study investigated the problem of alignment of the particles' heading directions. Reference [9] further provided theoretical characterization of [8] using graph theory and the notion of nearest neighbor rules.

Among all the papers concerning formation control of multi-agent systems, the most recent and closely related works to this paper are [10, 11] in which controllers are the emulation of injecting nonlinear springs and dampers between the agents. To ensure stability they considered the total energy with the potential function associated with the virtual nonlinear spring as a Lyapunov function and employ the Krasovskii-LaSalle invariance principle to guarantee asymptotic stability.

Following their control strategy in [10, 11], in this paper we consider a formation control problem of mobile multiple agents with sampled information; that is, each agent can communicate with other agents not continually but periodically. In particular, we focus our attention on the relationship between the sampling period, structure of the communication network, and the control performance. First, we discretize the equations of motion of the point-mass agents and introduce an energy-like function that is averaged over the sampling period. This function allows us to easily determine the feedback gains given a sampling period and a network connection topology. Then we examine the closed-loop system performance correlated with the energy dissipation rate.

The notation used in this paper is fairly standard. Specifically, \mathbb{R} denotes the set of real numbers, \mathbb{R}^n denotes the set of $n \times 1$ real column vectors, and \mathbb{N}_0 denotes the set of nonnegative integers. Furthermore, we write $(\cdot)^T$ for transpose, $A_{(i,j)}$ for the (i, j) th (block) element of the matrix A , 0_n for the n -dimensional square zero matrix, 1_n for the ones vector of dimension n , $\text{mspec}(A)$ for the spectrum of the matrix A , and $|\mathcal{N}_i|$ for the cardinal number of the set \mathcal{N}_i .

2 Motivation and Problem Settings

2.1 Continuous-Time Setting [10, 11]

In this section we introduce a formation control problem of multi-agent systems. Specifically, each agent is assumed to be a normalized point mass

and is subject to the force input. For simplicity of exposition, we assume that the agents are collision-free and allowed to move in a one-dimensional space. The extension to multi-dimensional systems is straightforward. Furthermore, we assume that the communication network is connected so that there is no information-isolated agents and the network topology is invariant over time. The control objective is to regulate each agent's position and velocity such that all the agents asymptotically travel with zero relative positions and common velocities.

To this end, consider the dynamics of n agents given by

$$\begin{aligned}\dot{q}(t) &= p(t), & q(0) &= q_0, & t &\geq 0, \\ \dot{p}(t) &= u(t), & p(0) &= p_0,\end{aligned}\tag{1}$$

where $q \triangleq [q_1, \dots, q_n]^T$, $p \triangleq [p_1, \dots, p_n]^T$, $u \triangleq [u_1, \dots, u_n]^T$, $q_i \in \mathbb{R}$, $p_i \in \mathbb{R}$, and $u_i \in \mathbb{R}$ are the position, the velocity, and the force input, respectively, of the i th agent.

In the preceding work [10, 11], the authors considered an energy-based controller that emulates forces due to springs and dampers in the continuous-time setting. In particular, their control law has the form of

$$u_i(t) = - \sum_{j \in \mathcal{N}_i} (q_i(t) - q_j(t)) - \sum_{j \in \mathcal{N}_i} (p_i(t) - p_j(t)), \quad i = 1, \dots, n,\tag{2}$$

or, equivalently,

$$u(t) = -Lq(t) - Lp(t),\tag{3}$$

where the first term on the right-hand side is induced as a gradient of the potential function $\phi(q) = \frac{1}{2}q^T Lq$ associated with the virtual spring with the stiffness coefficient matrix L , the second term plays a role of the damper with the damping coefficient matrix L , and \mathcal{N}_i represents the index set of the agents that the agent i is connected with. This symmetric, nonnegative-definite matrix L , called Laplacian in the field of graph theory, is determined from the structure of the communication network and has a simple zero eigenvalue since we assume that the network topology is connected (see Appendix A for details). Stability of the multi-agent system was guaranteed using the virtual energy (Lyapunov-like) function $V(q, p)$ given by

$$V(q, p) = \frac{1}{2}(p^T p + q^T Lq),\tag{4}$$

and the Krasovskii-LaSalle invariance principle.

2.2 Sampled-Data Setting

In this paper, we consider a more practical case than the continuous-time setting presented above. In particular, we assume that each controller can

simultaneously receive the information of relative positions and relative velocities of the agents prescribed by \mathcal{N}_i with time interval T . This synchronized intermittent information exchange naturally leads us to a formulation of sampled-data control.

For applying control, we employ zero-order hold so that the control input between the sampling instants is given by

$$u_i(t) = u_i[k], \quad kT \leq t < (k+1)T, \quad k \in \mathbb{N}_0, \quad i = 1, \dots, n, \quad (5)$$

where $u_i[k]$ denotes the input signal of the i th agent computed at the k th sampling instant $t = kT$. In this case, discretizing the equations of motion (1) with sampling period T , we obtain

$$\begin{aligned} q_i[k+1] &= q_i[k] + Tp_i[k] + \frac{1}{2}T^2u_i[k], & q_i[0] &= q_{i0}, & k &\in \mathbb{N}_0, \\ p_i[k+1] &= p_i[k] + Tu_i[k], & p_i[0] &= p_{i0}, \\ & & & & i &= 1, \dots, n, \end{aligned} \quad (6)$$

where $q_i[k]$ (resp., $p_i[k]$) represents the position (resp., velocity) of the i th agent at the k th sampling instant.

As one can surmise, the control input (5) with

$$u[k] = -k_q Lq[k] - k_p Lp[k], \quad (7)$$

where k_q, k_p are positive constants, can stabilize the multi-agent system in the case where the sampling period T is sufficiently small. Conversely, the input signal (7) with $k_q = k_p = 1$, which is inspired from (3), may destabilize the closed-loop system for a large sampling period. However, it is not obvious how small T should be to stabilize the system when the Laplacian matrix L and the positive constants k_q, k_p are given. In the following sections, we consider k_q, k_p as free parameters (or part of feedback gains) and derive sufficient conditions to answer this question. In addition, we further examine the relationship between the information exchange characteristics and control performance.

3 Single Agent Case

As a preliminary analysis of the multi-agent system, in this section we consider the problem of stabilizing a *single* agent (i.e., $n = 1$) to the origin with sampled information. Specifically, with sampling period T and the sampled-data control law (7), the closed-loop system trajectory of (1), (5) is given by

$$\begin{aligned} q(t) &= q[k] + p[k]t + \frac{1}{2}u[k]t^2, & kT \leq t < (k+1)T, & \quad k \in \mathbb{N}_0, \\ p(t) &= p[k] + u[k]t, \end{aligned} \quad (8)$$

and hence at the sampling instants it follows that

$$\begin{bmatrix} q[k+1] \\ p[k+1] \end{bmatrix} = \begin{bmatrix} 1 - \frac{1}{2}k_q T^2 & T - \frac{1}{2}k_p T^2 \\ -k_q T & 1 - k_p T \end{bmatrix} \begin{bmatrix} q[k] \\ p[k] \end{bmatrix}, \quad k \in \mathbb{N}_0. \quad (9)$$

3.1 Stability Analysis

Note that unlike the continuous-time case, the ‘total energy’ of the agents given by

$$V_1(q[k], p[k]) = \frac{1}{2}(p^2[k] + k_q q^2[k]), \quad (10)$$

cannot be an appropriate positive-definite (Lyapunov) function to examine stability in the sampled-data case. To see this, consider the time difference of $V_1(q, p)$ between $(k+1)$ th and k th sampling instants. Then it follows that the energy difference along the closed-loop system trajectories is given by

$$V_1(q[k+1], p[k+1]) - V_1(q[k], p[k]) = - \begin{bmatrix} q[k] \\ p[k] \end{bmatrix}^T \Lambda_d \begin{bmatrix} q[k] \\ p[k] \end{bmatrix}, \quad (11)$$

where the entries of the matrix $\Lambda_d \in \mathbb{R}^{2 \times 2}$ are obtained as

$$\begin{aligned} \Lambda_{d(1,1)} &= -\frac{1}{8}k_q^3 T^4, \\ \Lambda_{d(1,2)} &= \Lambda_{d(2,1)} = -\frac{1}{4}k_q k_p T^2 + \frac{1}{4}k_q^2 T^3 - \frac{1}{8}k_q k_p T^4, \\ \Lambda_{d(2,2)} &= k_p T - \frac{1}{2}(k_p^2 + k_q)T^2 + \frac{1}{2}k_q k_p T^3 - \frac{1}{8}k_q k_p^2 T^4. \end{aligned}$$

Now, since the $(1, 1)$ -element of Λ_d is *always* negative for all $k_q > 0$ and $T > 0$, Λ_d cannot be positive definite and hence the energy-like function $V_1(q, p)$ given by (10) is not an appropriate Lyapunov function.

Instead, we consider the *averaged* energy function between the sampling instants given by

$$V_2(q[k], p[k]) = \frac{1}{2T} \int_0^T (p^2(t) + k_q q^2(t)) dt, \quad (12)$$

where $q(t)$ and $p(t)$ are given by (8). In this case, with the control signal (7), the averaged energy function (12) is written as

$$V_2(q[k], p[k]) = \begin{bmatrix} q[k] \\ p[k] \end{bmatrix}^T \Theta \begin{bmatrix} q[k] \\ p[k] \end{bmatrix}, \quad (13)$$

where the entries of the matrix $\Theta \in \mathbb{R}^{2 \times 2}$ are given by

$$\begin{aligned} \Theta_{(1,1)} &= k_q + \frac{1}{20}k_q^3 T^4, \\ \Theta_{(1,2)} &= \Theta_{(2,1)} \\ &= \frac{1}{6}k_q k_p T^2 - \frac{1}{8}k_q^2 T^3 + \frac{1}{20}k_q^2 k_p T^4, \\ \Theta_{(2,2)} &= 1 - k_p T + \frac{1}{3}(k_p^2 + k_q)T^2 - \frac{1}{4}k_q k_p T^3 + \frac{1}{20}k_q k_p^2 T^4. \end{aligned}$$

Now, it follows that the energy difference at the sampling instants along the closed-loop system trajectories is given by

$$V_2(q[k+1], p[k+1]) - V_2(q[k], p[k]) = - \begin{bmatrix} q[k] \\ p[k] \end{bmatrix}^T \Lambda_s \begin{bmatrix} q[k] \\ p[k] \end{bmatrix}, \quad (14)$$

where the entries of the matrix $\Lambda_s \in \mathbb{R}^{2 \times 2}$ are expressed as

$$\begin{aligned} \Lambda_{s(1,1)} &= \frac{4}{3}k_q^2k_pT^3 - \frac{1}{6}k_q^2(5k_q + 2k_p^2)T^4 + \frac{11}{60}k_q^3k_pT^5 - \frac{1}{40}k_q^3(2k_p^2 - 7k_q)T^6 \\ &\quad - \frac{1}{20}k_q^4k_pT^7 - \frac{1}{80}k_q^5T^8, \\ \Lambda_{s(1,2)} &= \Lambda_{s(2,1)} \\ &= -\frac{3}{2}k_qk_pT^2 + \frac{1}{6}k_q(5k_q + 9k_p^2)T^3 - \frac{1}{24}k_qk_p(17k_q + 8k_p^2)T^4 \\ &\quad - \frac{1}{240}k_q^2(57k_q - 44k_p^2)T^5 - \frac{1}{40}k_q^2k_p(2k_p^2 - 9k_q)T^6 \\ &\quad - \frac{1}{40}k_q^3(2k_p^2 - k_q)T^7 - \frac{1}{80}k_q^4k_pT^8, \\ \Lambda_{s(2,2)} &= 2k_pT - (k_q + 3k_p^2)T^2 + \frac{1}{3}k_p(5k_p^2 + 4k_q)T^3 \\ &\quad - \frac{1}{12}(4k_p^4 - 3k_q^2 + 7k_qk_p^2)T^4 - \frac{1}{120}k_qk_p(57k_q - 22k_p^2)T^5 \\ &\quad - \frac{1}{40}k_q(2k_p^4 - 11k_qk_p^2 + 2k_q^2)T^6 - \frac{1}{20}k_q^2k_p(k_p^2 - k_q)T^7 \\ &\quad - \frac{1}{80}k_q^3k_p^2T^8. \end{aligned}$$

If the sampling period T is sufficiently small, then the matrix Λ_s is approximated as

$$\Lambda_s \simeq \tilde{\Lambda}_s \triangleq \begin{bmatrix} \frac{4}{3}k_q^2k_pT^3 & -\frac{3}{2}k_qk_pT^2 \\ -\frac{3}{2}k_qk_pT^2 & 2k_pT \end{bmatrix}. \quad (15)$$

In fact, since the eigenvalues of $\tilde{\Lambda}_s$ are computed as

$$\frac{1}{2} \left\{ \left(\frac{4}{3}k_q^2k_pT^3 + 2k_pT \right) \pm \sqrt{\left(\frac{4}{3}k_q^2k_pT^3 + 2k_pT \right)^2 - \frac{5}{3}k_q^2k_p^2T^4} \right\},$$

which turn out to be both positive, it follows that $\tilde{\Lambda}_s$ is positive definite and hence the closed-loop system given by (1), (5) can be shown to be asymptotically stable using the averaged energy function (12) as a Lyapunov function. Finally, it is important to note that with the sufficiently small sampling period T , time difference of the averaged energy function is strictly negative so that, unlike the continuous-time case, it is not necessary to employ the Krasovskii-LaSalle invariance principle.

Illustrative Example. Consider the single-agent system (1) and the control input (5), (7) with zero-order hold. Note that with $k_q = 1$, $k_p = 1$, and $T = 1$, Λ_s in (14) is positive definite and hence the closed-loop system is asymptotically stable. Figure 1 shows the energy-like function $V_1(q(t), p(t))$

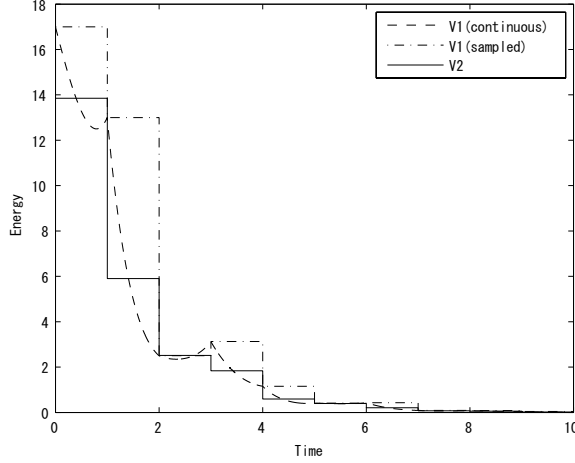


Figure 1: History of the virtual energy function (V_1) and the averaged energy function (V_2)

versus time (dashed line) for the case where $q(0) = 5$ and $p(0) = -3$. It can be seen that $V_1(q[k], p[k])$ is not a decreasing function of time kT , $k = \mathbb{N}_0$, (solid line) while the averaged energy function $V_2(q[k], p[k])$ is indeed decreasing at each sampling instant (dashed-dot line).

3.2 Relationship Between the Sampling Period and the Feedback Gains

As seen in Section 3.1, it follows that the single-agent system can be stabilized around the equilibrium point with sufficiently small sampling period T depending on the feedback gains k_q and k_p . In other words, for a fixed sampling period T , it is required to select appropriate feedback gains in order to stabilize the single-agent system. In this section, we derive sufficient conditions that k_q, k_p ought to satisfy for stabilization of the closed-loop single-agent system.

Let $\hat{k}_q \triangleq k_q T^2$ and $\hat{k}_p \triangleq k_p T$. Then the matrix Λ_s in (14) can be rewritten as

$$\Lambda_s = \begin{bmatrix} \frac{1}{T} & 0 \\ 0 & 1 \end{bmatrix} \Phi \begin{bmatrix} \frac{1}{T} & 0 \\ 0 & 1 \end{bmatrix}, \quad (16)$$

where the entries of the matrix $\Phi \in \mathbb{R}^{2 \times 2}$ are given by

$$\begin{aligned} \Phi_{(1,1)} &= -\frac{1}{3}\hat{k}_q^2\hat{k}_p(\hat{k}_p - 4) - \frac{1}{60}\hat{k}_q^3(50 - 11\hat{k}_p + 3\hat{k}_p^2) - \frac{1}{40}\hat{k}_q^4(2\hat{k}_p - 7) - \frac{1}{80}\hat{k}_q^5, \\ \Phi_{(1,2)} &= \Phi_{(2,1)} \\ &= -\frac{1}{6}\hat{k}_q\hat{k}_p(9 - 9\hat{k}_p + 2\hat{k}_p^2) - \frac{1}{120}\hat{k}_q^2(-100 + 85\hat{k}_p - 22\hat{k}_p^2 + 6\hat{k}_p^3) \\ &\quad - \frac{1}{240}\hat{k}_q^3(57 - 54\hat{k}_p + 12\hat{k}_p^2) - \frac{1}{80}\hat{k}_q^4(-2 + \hat{k}_p), \end{aligned}$$

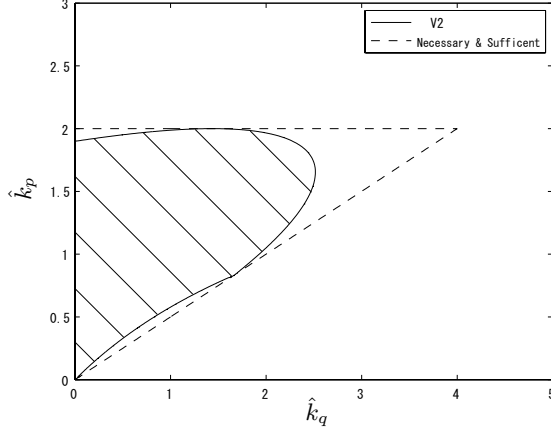


Figure 2: Stabilizing region of \hat{k}_q, \hat{k}_p . This region is nonconvex and does not depend on T .

$$\begin{aligned} \Phi_{(2,2)} = & 2\hat{k}_p - 3\hat{k}_p^2 + \frac{5}{3}\hat{k}_p^3 - \frac{1}{3}\hat{k}_p^4 - \frac{1}{60}\hat{k}_q(60 - 80\hat{k}_p + 35\hat{k}_p^2 - 11\hat{k}_p^3 + 3\hat{k}_p^4) \\ & - \frac{1}{120}\hat{k}_q^2(-30 + 57\hat{k}_p - 33\hat{k}_p^2 + 6\hat{k}_p^3) - \frac{1}{80}\hat{k}_q^3(4 - 4\hat{k}_p + \hat{k}_p^2). \end{aligned}$$

Note that the sampling period T does not explicitly appear in the expression of Φ . Figure 2 indicates the nonconvex region of \hat{k}_q and \hat{k}_p that makes Φ (and hence Λ_s) positive definite and thus the closed-loop system given by (1), (5) be asymptotically stable irrespective of T .

In summary, if the sampling period T is given, then the stabilizing feedback gains can be determined as

$$k_q = \frac{\hat{k}_q}{T^2}, \quad k_p = \frac{\hat{k}_p}{T}, \quad (17)$$

through the constants \hat{k}_q, \hat{k}_p that lie in the shaded region in Figure 2. Since the shaded region is bounded, it follows that if the sampling period is large, then the feedback gains need to be small to ensure stability. Finally, we note that the necessary and sufficient region of \hat{k}_q, \hat{k}_p is shown in Figure 2, which is directly derived from the condition that all the eigenvalues of the system matrix in (9) lie in the unit disk. Nonetheless, we emphasize that the use of Lyapunov-like analysis facilitates stability and performance analysis as we see in the following sections.

4 Stability Analysis for Multi-Agent Case

The discussion in the preceding section for the single-agent case indicates that the averaged energy function is likely to be a viable Lyapunov function

candidate for the multi-agent case as well. In this section, we employ a similar function to (12) to derive stabilizing region of k_q, k_p for constructing the control signal (7).

First, discretizing (1) with sampling period T and using the control input (5) with the control signal (7), it follows that the closed-loop system trajectory has the same expression as (8) and that the states $q(t)$ and $p(t)$ at the sampling instants are given by

$$\begin{bmatrix} q[k+1] \\ p[k+1] \end{bmatrix} = \begin{bmatrix} I_n - \frac{1}{2}k_qLT^2 & TI_n - \frac{1}{2}k_pLT^2 \\ -k_qLT & I_n - k_pLT \end{bmatrix} \begin{bmatrix} q[k] \\ p[k] \end{bmatrix}, \quad k \in \mathbb{N}_0. \quad (18)$$

Now, consider the averaged energy-like function

$$V_2(q[k], p[k]) = \frac{1}{2T} \int_0^T \{p^T(t)p(t) + k_q q^T(t)Lq(t)\} dt, \quad (19)$$

where $q(t)$ and $p(t)$ are given by (8). As in Section 3.1, it follows that the energy difference at the sampling instants along the closed-loop system trajectories is given by

$$V_2(q[k+1], p[k+1]) - V_2(q[k], p[k]) = - \begin{bmatrix} q[k] \\ p[k] \end{bmatrix}^T \hat{\Lambda}_s(L) \begin{bmatrix} q[k] \\ p[k] \end{bmatrix}, \quad (20)$$

where

$$\hat{\Lambda}_s(L) = \begin{bmatrix} \frac{1}{T}I_n & 0 \\ 0 & I_n \end{bmatrix} \hat{\Phi}(L) \begin{bmatrix} \frac{1}{T}I_n & 0 \\ 0 & I_n \end{bmatrix}, \quad (21)$$

and the block entries of the matrix $\hat{\Phi}(L) \in \mathbb{R}^{2n \times 2n}$ are given by

$$\begin{aligned} \hat{\Phi}_{(1,1)}(L) &= -\frac{1}{6}\hat{k}_q^2(5\hat{k}_q - 8\hat{k}_p)L^3 - \frac{1}{120}\hat{k}_q^2(-21\hat{k}_q^2 - 22\hat{k}_q\hat{k}_p + 40\hat{k}_p^2)L^4 \\ &\quad - \frac{1}{80}\hat{k}_q^3(\hat{k}_q^2 + 4\hat{k}_q\hat{k}_p + 4\hat{k}_p^2)L^5, \\ \hat{\Phi}_{(1,2)}(L) &= \hat{\Phi}_{(2,1)}(L) \\ &= -\frac{1}{6}\hat{k}_q(-5\hat{k}_q + 9\hat{k}_p)L^2 - \frac{1}{240}\hat{k}_q(57\hat{k}_q^2 + 170\hat{k}_q\hat{k}_p - 360\hat{k}_p^2)L^3 \\ &\quad - \frac{1}{120}\hat{k}_q(-3\hat{k}_q^3 - 27\hat{k}_q^2\hat{k}_p - 22\hat{k}_q\hat{k}_p^2 + 40\hat{k}_p^3)L^4 \\ &\quad - \frac{1}{80}\hat{k}_q^2\hat{k}_p(\hat{k}_q^2 + 4\hat{k}_q\hat{k}_p + 4\hat{k}_p^2)L^5, \\ \hat{\Phi}_{(2,2)}(L) &= -(\hat{k}_q - 2\hat{k}_p)L - \frac{1}{12}(-3\hat{k}_q^2 - 16\hat{k}_q\hat{k}_p + 36\hat{k}_p^2)L^2 \\ &\quad - \frac{1}{120}(6\hat{k}_q^3 + 57\hat{k}_q^2\hat{k}_p + 70\hat{k}_q\hat{k}_p^2 - 200\hat{k}_p^3)L^3 \\ &\quad - \frac{1}{120}\hat{k}_p(-6\hat{k}_q^3 - 33\hat{k}_q^2\hat{k}_p - 22\hat{k}_q\hat{k}_p^2 + 40\hat{k}_p^3)L^4 \\ &\quad - \frac{1}{80}\hat{k}_q\hat{k}_p^2(\hat{k}_q^2 + 4\hat{k}_q\hat{k}_p + 4\hat{k}_p^2)L^5. \end{aligned} \quad (22)$$

In order to examine the sign definiteness of $\hat{\Phi}(L)$, we present the following lemma to recall the Frobenius' (spectral mapping) theorem [12]. For the

statement of the following results, let $0 = \lambda_1 < \lambda_2 \leq \dots \leq \lambda_n$ be the eigenvalues of the Laplacian L .

Frobenius' Spectral Mapping Theorem [12]. Consider a matrix $A \in \mathbb{R}^{n \times n}$ and a polynomial $m(s)$ of s . Let $\lambda \in \text{mspec}(A)$ and $v \in \mathbb{R}^n$ be the corresponding eigenvector. Then $m(\lambda) \in \text{mspec}(m(A))$ and v is the corresponding eigenvector of $m(A)$.

Lemma 4.1 *Let $L \in \mathbb{R}^{n \times n}$ be a Laplacian matrix and let $m_{ij}(s)$, $i, j = 1, 2$, be polynomials of s . Furthermore, let $\lambda_k \in \text{mspec}(L)$, $k = 1, \dots, n$. Then the $2n$ eigenvalues of the matrix*

$$M(L) \triangleq \begin{bmatrix} m_{11}(L) & m_{12}(L) \\ m_{21}(L) & m_{22}(L) \end{bmatrix} \in \mathbb{R}^{2n \times 2n}, \quad (23)$$

are identical to the roots of n second-order algebraic equations of z given by

$$z^2 - (m_{11}(\lambda_k) + m_{22}(\lambda_k))z + m_{11}(\lambda_k)m_{22}(\lambda_k) - m_{12}(\lambda_k)m_{21}(\lambda_k) = 0, \quad k = 1, \dots, n. \quad (24)$$

Proof. Since L is diagonalizable, it follows from the Jordan decomposition and the spectral mapping theorem that there exists a nonsingular matrix $Q \in \mathbb{R}^{n \times n}$ composed of the eigenvectors of L such that

$$L = Q^{-1} \begin{bmatrix} \lambda_1 & & \\ & \ddots & \\ & & \lambda_n \end{bmatrix} Q. \quad (25)$$

Furthermore, letting $R \triangleq \text{block-diag}[Q, Q]$, it follows that

$$M(L) = R^{-1} \begin{bmatrix} m_{11}(\lambda) & m_{12}(\lambda) \\ m_{21}(\lambda) & m_{22}(\lambda) \end{bmatrix} R, \quad (26)$$

where $m_{ij}(\lambda) \triangleq \text{diag}[m_{ij}(\lambda_1), \dots, m_{ij}(\lambda_n)] \in \mathbb{R}^{n \times n}$, $i, j = 1, 2$. Now, since the eigenvalues of $M(L)$ are the same as those of $\begin{bmatrix} m_{11}(\lambda) & m_{12}(\lambda) \\ m_{21}(\lambda) & m_{22}(\lambda) \end{bmatrix}$ composed of diagonal matrices, it follows that the eigenvalues of $M(L)$ are the roots of (24). \square

It follows from the fact that $\hat{\Phi}(\lambda_1) = \hat{\Phi}(0) = 0_2$ and Lemma 4.1 that the necessary and sufficient conditions for $\hat{\Phi}(L)$ to be nonnegative definite are

$$\hat{\Phi}_{11}(\lambda_i) + \hat{\Phi}_{22}(\lambda_i) > 0, \quad \hat{\Phi}_{11}(\lambda_i)\hat{\Phi}_{22}(\lambda_i) - \hat{\Phi}_{12}^2(\lambda_i) > 0, \quad (27)$$

for all $i = 2, \dots, n$. Following the similar argument as in the case of single agent (Section 3), define $\tilde{k}_q \triangleq \lambda_i \hat{k}_q$ and $\tilde{k}_p \triangleq \lambda_i \hat{k}_p$ so that $\hat{\Phi}(\lambda_i)$ is given by (17) with \hat{k}_q, \hat{k}_p replaced by \tilde{k}_q, \tilde{k}_p , respectively. This implies that the transformed gains $\tilde{k}_q (= \lambda_i \hat{k}_q)$ and $\tilde{k}_p (= \lambda_i \hat{k}_p)$ ought to lie in the *nonconvex*

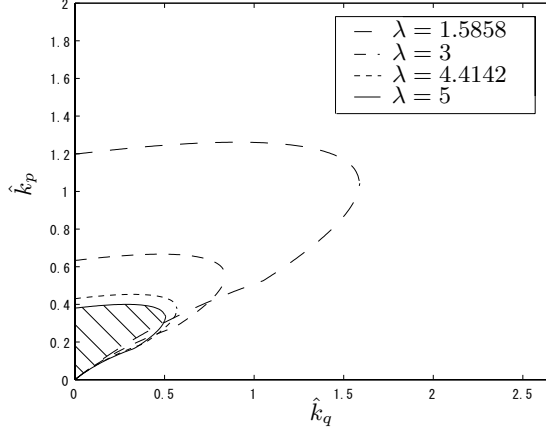


Figure 3: Stabilizing region of \hat{k}_q, \hat{k}_p in the case where L has eigenvalues $\lambda = 1.5858, 3, 4.4142, 5$. Each curve is homothetic to the one in Figure 2 with ratio $1/\lambda$ with respect to the origin.

set indicated in Figure 2 for all $i = 2, \dots, n$, and hence \hat{k}_q, \hat{k}_p should be contained in the shaded region in Figure 3. (Each curve is homothetic to the one in Figure 2 with ratio $1/\lambda$ with respect to the origin.) One of the simple ways to determine a stabilizing gain is to consider the region specified in Figure 4. Note that the straight line that goes from the origin is the line tangent to the concave curve at the origin. In fact, the slope of the line is numerically computed to be 0.7633. Furthermore, the largest eigenvalue λ_n of L characterizes the size of the region in Figure 3. Now, since $\tilde{k}_q = \lambda_n \hat{k}_q = \lambda_n k_q T^2$ and $\tilde{k}_p = \lambda_n \hat{k}_p = \lambda_n k_p T$, take any point in the shaded region in Figure 4 to obtain the stabilizing gains

$$k_q = \frac{\tilde{k}_q}{\lambda_n T^2}, \quad k_p = \frac{\tilde{k}_p}{\lambda_n T}, \quad (28)$$

using the largest eigenvalue of L .

At the end of the section of stability analysis, we summarize the results discussed above in the following theorem.

Theorem 4.1 *Consider the multi-agent system given by (1), where the sampling period T and the Laplacian matrix L associated with the communication network are predetermined. Suppose that the feedback gains k_q, k_p are given by (28), where \tilde{k}_q, \tilde{k}_p are selected from the region indicated in Figure 4. Then the control law (5), (7) guarantees that the closed-loop multi-agent system (1) satisfies*

$$\lim_{t \rightarrow \infty} |q_i(t) - q_j(t)| = 0, \quad \lim_{t \rightarrow \infty} |p_i(t) - p_j(t)| = 0, \quad (29)$$

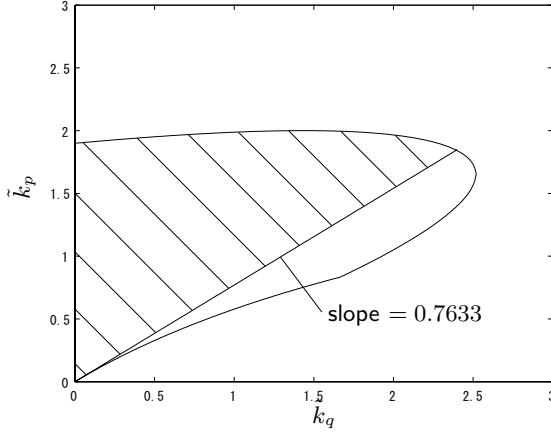


Figure 4: Simplified stabilizing region of \tilde{k}_q, \tilde{k}_p

for all $i, j = 1, \dots, n$.

Proof. The proof is similar to the discussion in Section 3. Specifically, with the control signal (7) and the feedback gains obtained in (28), we saw that the time difference of the averaged energy-like function $V_2(q[k], p[k])$ given by (13) along the closed-loop system trajectories satisfies

$$V_2(q[k+1], p[k+1]) - V_2(q[k], p[k]) = - \begin{bmatrix} q[k] \\ p[k] \end{bmatrix}^T \hat{\Lambda}_s(L) \begin{bmatrix} q[k] \\ p[k] \end{bmatrix} \leq 0, \quad (30)$$

and hence the vector $[q^T[k], p^T[k]]^T$ converges to the null space of $\hat{\Lambda}_s(L)$, which is given by $[r_q \mathbf{1}_n^T, r_p \mathbf{1}_n^T]^T$, where $r_p, r_q \in \mathbb{R}$. Hence, it follows that all the agents asymptotically move with the same velocities and zero relative positions. \square

It follows from Theorem 4.1 that $u[k] \rightarrow 0$ as $k \rightarrow \infty$ and hence $p[k+1] - p[k] \rightarrow 0$ as $k \rightarrow \infty$. Furthermore, note that $V_2(q[k], p[k])$ is a decreasing function of k and hence $p[k]$ is bounded. Now, since $p[k]$ is a bounded Cauchy sequence, it follows that there exists a constant $p_{ss} \in \mathbb{R}$ such that $p(t) \rightarrow p_{ss} \mathbf{1}_n$ as $t \rightarrow \infty$. Finally, $\tilde{\Lambda}_s(L)$ has two semisimple eigenvalues, one of which corresponds to the rigid-body mode of the system.

5 Performance Analysis for Multi-Agent Case

As discussed in Appendix A, eigenvalues of Laplacian matrices tend to become larger as there are more connections between agents. To evaluate performance with respect to the communication rate T and the network structure L , we ‘normalize’ the control input such that the control input is

given by (7) with i th input signal divided by the number of agents that the i th agent can communicate with; that is, we consider the control input given by

$$u_i[k] = -\frac{k_q}{|\mathcal{N}_i|} \sum_{j \in \mathcal{N}_i} (q_i[k] - q_j[k]) - \frac{k_p}{|\mathcal{N}_i|} \sum_{j \in \mathcal{N}_i} (p_i[k] - p_j[k]), \quad i = 1, \dots, n, \quad (31)$$

or, equivalently,

$$u[k] = -k_q \hat{M}^{-1} L q[k] - k_p \hat{M}^{-1} L p[k], \quad (32)$$

where $\hat{M} \triangleq \text{diag}[|\mathcal{N}_1|, \dots, |\mathcal{N}_n|]$.

In fact, when the feedback gains k_q, k_p are chosen properly, the closed-loop system under this setup remains stable, which can be shown by considering the modified energy-like function

$$V_3(q[k], p[k]) = \frac{1}{2T} \int_0^T \{p^T(t) \hat{M} p(t) + k_q q^T(t) L q(t)\} dt, \quad (33)$$

and by following the similar argument as in Section 4. Specifically, time difference of the energy-like function along the closed-loop trajectories is given by

$$V_3(q[k+1], p[k+1]) - V_3(q[k], p[k]) = - \begin{bmatrix} q[k] \\ p[k] \end{bmatrix}^T \tilde{\Lambda}_s(L) \begin{bmatrix} q[k] \\ p[k] \end{bmatrix}, \quad (34)$$

where

$$\tilde{\Lambda}_s(L) = \begin{bmatrix} \frac{1}{T} \hat{M}^{\frac{1}{2}} & 0 \\ 0 & \hat{M}^{\frac{1}{2}} \end{bmatrix} \tilde{\Phi}(\tilde{L}) \begin{bmatrix} \frac{1}{T} \hat{M}^{\frac{1}{2}} & 0 \\ 0 & \hat{M}^{\frac{1}{2}} \end{bmatrix}, \quad (35)$$

$\hat{M}^{\frac{1}{2}} \triangleq \text{diag}[|\mathcal{N}_1|^{\frac{1}{2}}, \dots, |\mathcal{N}_n|^{\frac{1}{2}}]$, $\tilde{L} \triangleq M^{-\frac{1}{2}} L M^{-\frac{1}{2}}$ and the block entries of the matrix $\tilde{\Phi}(\tilde{L}) \in \mathbb{R}^{2n \times 2n}$ are given by the same expression of $\hat{\Phi}(L)$ as in (22) with L replaced by \tilde{L} . The matrix \tilde{L} is referred to as the *normalized Laplacian matrix* [13].

Thus, similarly to Theorem 4.1, the control law (7) with the feedback gains given by (28) with λ_n replaced by the largest eigenvalue $\tilde{\lambda}_n$ of \tilde{L} , it follows that the closed-loop system (1), (5), (32) satisfies (29). Note that we assume the communication network is connected, and hence $\hat{M} \geq I_n$, which leads to $\tilde{\lambda}_n \leq \lambda_n$.

Finally, we evaluate the closed-loop system performance by an eigenvalue of $\tilde{\Lambda}_s(L)$. In particular, we focus on the smallest, nonzero eigenvalue λ^* of $\tilde{\Lambda}_s(L)$, since it characterizes the lowest convergence rate of the system. This eigenvalue is particularly called the algebraic connectivity. Figure 5 shows λ^* of the complete graph, the path graph and Graph A, which we define as a path graph with extra connections with second next agents added, in

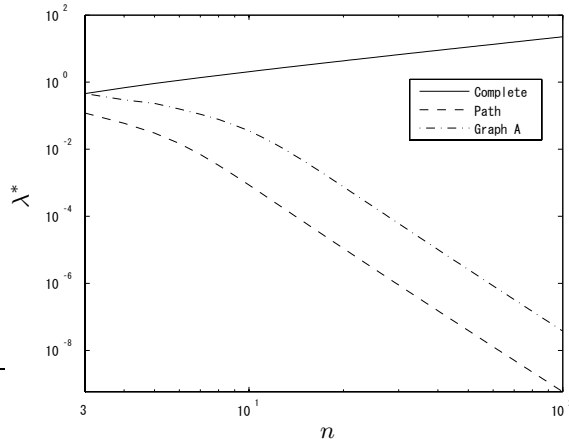


Figure 5: Smallest, nonzero eigenvalue λ^* of $\tilde{\Lambda}_s(L)$ of the complete graph, the path graph, and Graph A defined in Appendix A in the case of $\tilde{k}_q = \tilde{k}_p = 1.5$ and $T = 0.1$.

the case where \tilde{k}_q and \tilde{k}_p are kept constant (see Figure 6 in Appendix A for graphical representation of the complete and the path graphs and Graph A). While λ^* of the path graph and Graph A decrease as the number of agents increases, λ^* of the complete graph increases. This implies that the more information is available, the faster the convergence rate is.

6 Conclusion

In this paper we considered a sample-data control framework for formation control of multi-agent systems. Our zero-order hold controller resembles that of [10, 11], in which the control law was inspired by the energy dissipation of mass-spring-damper systems. Based on a stability analysis for the single-agent case, we derived explicit stability conditions in terms of the sampling period and the topology of the communication network using an averaged energy-like function. Finally, we provided a relationship between the network structure and control performance. Future research includes introducing system noise so that how accuracy of the available information affects the system performance.

References

- [1] C. Tomlin, G. Pappas, and S. Sastry, “Conflict resolution for air traffic management: a study in multiagent hybrid systems,” *IEEE Trans. Autom. Contr.*, vol. 43, no. 4, pp. 509–521, 1998.

- [2] J. Z. Hernández, S. Ossowski, and A. García-Serrano, “Multiagent architectures for intelligent traffic management systems,” *Transportation Research Part C: Emerging Technologies*, vol. 10, no. 5–6, pp. 473–506, 2002.
- [3] E. Pagello, A. D’Angeloc, F. Monteselloa, F. Garellia, and C. Ferraria, “Cooperative behaviors in multi-robot systems through implicit communication,” *Robotics and Autonomous Systems*, vol. 29, no. 1, pp. 65–77, 1999.
- [4] P. Silvestrin, “Control and navigation aspects of the new Earth observation missions of the European Space Agency,” *Annual Reviews in Control*, vol. 29, no. 2, pp. 247–260, 2005.
- [5] RoboCup Official Site, <http://www.robocup.org/>
- [6] J. A. Fax and R. M. Murray, “Information flow and cooperative control of vehicle formations,” *IEEE Trans. Autom. Contr.*, vol. 49, no. 9, pp. 1465–1476, 2004.
- [7] C. W. Reynolds, “Flocks, herds, and schools: A distributed behavioral model,” *Computer Graphics*, vol. 21, no. 4, pp. 25–34, 1987.
- [8] T. Vicsek, A. Czirok, E. Ben-Jacobs, I. Cohen, and O. Shochet, “Novel type of phase transition in a system of self-driven particles,” *Physical Review Letters*, vol. 75, no. 6, pp. 1226–1229, 1995.
- [9] A. Jadbabaie, J. Lin, and A. S. Morse, “Coordination of groups of mobile autonomous agents using nearest neighbor rules,” *Physical Review Letters*, vol. 48, no. 6, pp. 988–1001, 2003.
- [10] H. G. Tanner, A. Jadbabaie, and G. J. Papas, “Stable flocking of mobile agents, part I: Fixed topology,” in *Proc. IEEE Conf. Dec. Contr.*, (Maui, HI), pp. 2010–2015, December 2003.
- [11] H. G. Tanner, A. Jadbabaie, and G. J. Papas, “Stable flocking of mobile agents, part II: Dynamic topology,” in *Proc. IEEE Conf. Dec. Contr.*, (Maui, HI), pp. 2016–2020, December 2003.
- [12] P. D. Lax, *Linear Algebra*. New York, NY: John Wiley & Sons, 1996.
- [13] F. R. K. Chung, *Spectral Graph Theory*. Providence, RI: American Mathematical Society, 1997.
- [14] Z. Lin, B. Francis, and M. Maggiore, “Necessary and sufficient graphical conditions for formation control of unicycles,” *IEEE Trans. Autom. Contr.*, vol. 50, no. 1, pp. 121–127, 2005.
- [15] C. Godsil and G. Royle, *Algebraic Graph Theory*. New York, NY: Springer-Verlag, 2001.

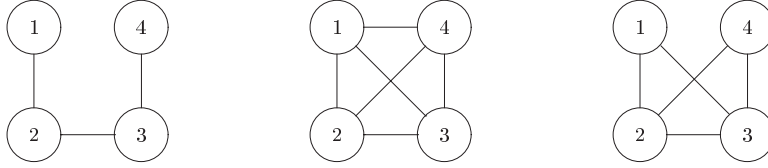


Figure 6: Path graph (left), complete graph (center), and Graph A (right) in the case of 4-agent systems

Appendix

A Properties of the Laplacian Matrix

In describing the structure of information exchange between the agents, graph theory plays a crucial role and provides useful insights that lead to stability analyses [14]. Specifically, in this appendix we focus on the definition of Laplacian matrix and some of its important properties necessary for this paper.

Suppose that the agent i and the agent j ($\neq i$) out of n agents have a common communication channel (i.e., if $i \in \mathcal{N}_j$, then $j \in \mathcal{N}_i$) so that the agents i and j know each other's relative position and/or velocity. This communication network can be characterized via the Laplacian matrix L defined by

$$L_{(i,j)} = \begin{cases} -1, & i \in \mathcal{N}_j, \\ |\mathcal{N}_i|, & j = i, \\ 0, & \text{otherwise,} \end{cases} \quad i, j = 1, \dots, n. \quad (36)$$

Thus, the Laplacian matrix is a symmetric matrix. Furthermore, the Laplacian matrix has the following properties [15]: (i) The eigenvalues of L are all (real and) nonnegative. (ii) If L is irreducible (i.e., the undirected graph associated with L is complete), then L has only one simple zero eigenvalue and the corresponding eigenvector is given by $\mathbf{1}_n$.

Finally, we define two special types of graphs that are considered in Section 5. Specifically, Figure 6 shows the complete graph, the path graph, and Graph A in the case of 4-agent systems.